

Maximum Power Point Tracking (MPPT) Of Solar Cell Using Buck-Boost Converter

Sunil Kumar Mahapatro

Asst. Prof., E.E.E. dept.

Gandhi Institute For Technology

Bhubaneswar, Odisha, India

Abstract:

The need for renewable energy sources is on the rise because of the acute energy crisis in the world today. India plans to produce 20 Gigawatts Solar power by the year 2020, whereas we have only realized less than half a Gigawatt of our potential as of March 2010. Solar energy is a vital untapped resource in a tropical country like ours. The main hindrance for the penetration and reach of solar PV systems is their low efficiency and high capital cost. In this paper utilization of a buck-boost converter for control of photovoltaic power using Maximum Power Point Tracking (MPPT) control mechanism is presented. For the main aim of the project the boost converter is to be used along with a Maximum Power Point Tracking control mechanism. The MPPT is responsible for extracting the maximum possible power from the photovoltaic and feed it to the load via the buck-boost converter which steps up the voltage to required magnitude. The main aim will be to track the maximum power point of the photovoltaic module so that the maximum possible power can be extracted from the photovoltaic. In this thesis, we examine a schematic to extract maximum obtainable solar power from a PV module and use the energy for a DC application. This project investigates in detail the concept of Maximum Power Point Tracking (MPPT) which significantly increases the efficiency of the solar photovoltaic system.

1. Introduction

1.1 The need for Renewable Energy

Renewable energy is the energy which comes from natural resources such as sunlight, wind, rain, tides and geothermal heat. These resources are renewable and can be naturally replenished. Therefore, for all practical purposes, these resources can be considered to be inexhaustible, unlike dwindling conventional fossil fuels [1]. The global energy crunch has provided a renewed impetus to the growth and development of Clean and Renewable Energy sources. Clean Development Mechanisms (CDMs) [2] are being adopted by organizations all across the globe.

Apart from the rapidly decreasing reserves of fossil fuels in the world, another major factor working against fossil fuels is the pollution associated with their combustion. Contrastingly, renewable energy sources are known to be much cleaner and produce energy without the harmful effects of pollution unlike their conventional counterparts.

1.2 Different sources of Renewable Energy

1.2.1 Wind power

Wind turbines can be used to harness the energy [3] available in airflows. Current day turbines range from around 600 kW to 5 MW [4] of rated power. Since the power output is a function of the cube of the wind speed, it increases rapidly with an increase in available wind velocity. Recent advancements have led to aerofoil wind turbines, which are more efficient due to a better aerodynamic structure.

1.2.2 Solar power

The tapping of solar energy owes its origins to the British astronomer John Herschel [5] who famously used a solar thermal collector box to cook food during an expedition to Africa. Solar energy can be utilized in two major ways. Firstly, the captured heat can be used as solar thermal energy, with applications in space heating. Another alternative is the conversion of incident solar radiation to electrical energy, which is the most usable form of energy. This can be achieved with the help of solar photovoltaic cells [6] or with concentrating solar power plants.

1.2.3 Small hydropower

Hydropower installations up to 10MW are considered as small hydropower and counted as renewable energy sources [7]. These involve converting the potential energy of water stored in dams into usable electrical energy through the use of water turbines. Run-of-the-river hydroelectricity aims to utilize the kinetic energy of water without the need of building reservoirs or dams.

1.2.4 Biomass

Plants capture the energy of the sun through the process of photosynthesis. On combustion, these plants release the trapped energy. This way, biomass

works as a natural battery to store the sun's energy [8] and yield it on requirement.

1.2.5 Geothermal

Geothermal energy is the thermal energy which is generated and stored [9] within the layers of the Earth. The gradient thus developed gives rise to a continuous conduction of heat from the core to the surface of the earth. This gradient can be utilized to heat water to produce superheated steam and use it to run steam turbines to generate electricity. The main disadvantage of geothermal energy is that it is usually limited to regions near tectonic plate boundaries, though recent advancements have led to the propagation of this technology [10].

1.3 Renewable Energy trends across the globe

The current trend across developed economies tips the scale in favour of Renewable Energy. For the last three years, the continents of North America and Europe have embraced more renewable power capacity as compared to conventional power capacity. Renewable accounted for 60% of the newly installed power capacity in Europe in 2009 and nearly 20% of the annual power production [7].

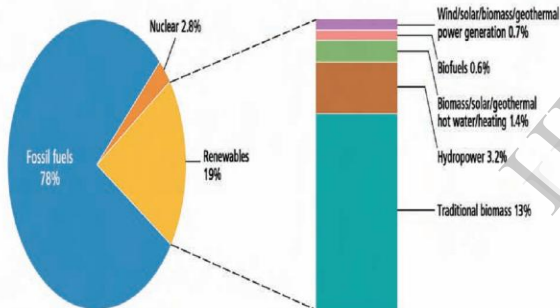


Figure 1: Global energy consumption in year 2011

As can be seen from the figure-1, wind and biomass occupy a major share of the current renewable energy consumption. Recent advancements in solar photovoltaic technology and constant incubation of projects in countries like Germany and Spain have brought around tremendous growth in the solar PV market as well, which is projected to surpass other renewable energy sources in the coming years.

By 2009, more than 85 countries had some policy target to achieve a predetermined share of their power capacity through renewables. This was an increase from around 45 countries in 2005. Most of the targets are also very ambitious, landing in the range of 30-90% share of national production through renewables. Noteworthy policies are the European Union's target of achieving 20% of total energy through renewables by 2020 and India's Jawaharlal

Nehru Solar Mission, through which India plans to produce 20GW solar energy by the year 2022.

2. Solar Cell

2.1 Operating principle

Solar cells are the basic components of photovoltaic panels. Most are made from silicon even though other materials are also used.

Solar cells take advantage of the photoelectric effect: the ability of some semiconductors to convert electromagnetic radiation directly into electrical current. The charged particles generated by the incident radiation are separated conveniently to create an electrical current by an appropriate design of the structure of the solar cell, as will be explained in brief below.

A solar cell is basically a p-n junction which is made from two different layers of silicon doped with a small quantity of impurity atoms: in the case of the n-layer, atoms with one more valence electron, called donors, and in the case of the p-layer, with one less valence electron, known as acceptors. When the two layers are joined together, near the interface the free electrons of the n-layer are diffused in the p-side, leaving behind an area positively charged by the donors. Similarly, the free holes in the p-layer are diffused in the n-side, leaving behind a region negatively charged by the acceptors. This creates an electrical field between the two sides that is a potential barrier to further flow. The equilibrium is reached in the junction when the electrons and holes cannot surpass that potential barrier and consequently they cannot move. This electric field pulls the electrons and holes in opposite directions so the current can flow in one way only: electrons can move from the p-side to the n-side and the holes in the opposite direction. A diagram of the p-n junction showing the effect of the mentioned electric field is illustrated in Figure 2.

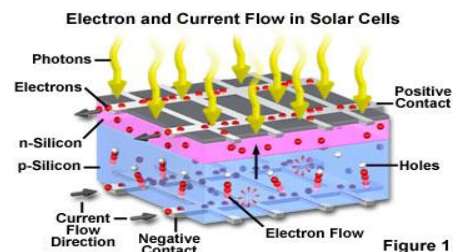


Figure 2: Solar cell

Metallic contacts are added at both sides to collect the electrons and holes so the current can flow. In the case of the n-layer, which is facing the solar

irradiance, the contacts are several metallic strips, as they must allow the light to pass to the solar cell, called fingers.

The structure of the solar cell has been described so far and the operating principle is next. The photons of the solar radiation shine on the cell. Three different cases can happen: some of the photons are reflected from the top surface of the cell and metal fingers. Those that are not reflected penetrate in the substrate. Some of them, usually the ones with less energy, pass through the cell without causing any effect. Only those with energy level above the band gap of the silicon can create an electron-hole pair. These pairs are generated at both sides of the p-n junction. The minority charges (electrons in the p-side, holes in the n-side) are diffused to the junction and swept away in opposite directions (electrons towards the n-side, holes towards the p-side) by the electric field, generating a current in the cell, which is collected by the metal contacts at both sides. This can be seen in the figure above, Figure 2. This is the light-generated current which depends directly on the irradiation: if it is higher, then it contains more photons with enough energy to create more electron-hole pairs and consequently more current is generated by the solar cell.

2.2 Equivalent circuit of a solar cell

The solar cell can be represented by the electrical model shown in Figure 3. Its current voltage characteristic is expressed by the following equation:

$$I = I_L - I_0 \left\{ \exp \left[\frac{q(V + IR_S)}{nkT} \right] - 1 \right\} - \frac{V + IR_S}{R_{SH}} \tag{1}$$

Where I and V are the solar cell output current and voltage respectively, I₀ is the dark saturation current, q is the charge of an electron, A is the diode quality (ideality) factor, k is the Boltzmann constant, T is the absolute temperature and R_S and R_{SH} are the series and shunt resistances of the solar cell. R_S is the resistance offered by the contacts and the bulk semiconductor material of the solar cell. The origin of the shunt resistance R_{SH} is more difficult to explain. It is related to the non ideal nature of the p-n junction and the presence of impurities near the edges of the cell that provide a short-circuit path around the junction [4]. In an ideal case R_S would be zero and R_{SH} infinite. However, this ideal scenario is not possible and manufacturers try to minimize the effect of both resistances to improve their products.

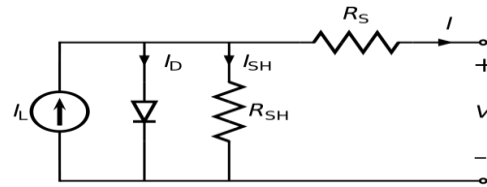


Figure 3: Equivalent circuit of a solar cell

Sometimes, to simplify the model, the effect of the shunt resistance is not considered, i.e. R_{SH} is infinite, so the last term in equation (1) is neglected.

2.3 Open circuit voltage, short circuit current and maximum power point

Two important points of the current-voltage characteristic must be pointed out: the open circuit voltage V_{OC} and the short circuit current I_{SC}. At both points the power generate is zero. V_{OC} can be approximated from (1) when the output current of the cell is zero, i.e. I=0 and the shunt resistance R_{SH} is neglected. It is represented by equation (2). The short circuit current I_{SC} is the current at V = 0 and is approximately equal to the light generated current I_L as shown in equation (3).

$$V_{OC} \approx \frac{nkT}{q} \ln \left(\frac{I_L}{I_0} + 1 \right) \tag{2}$$

$$I_{SC} \approx I_L \tag{3}$$

The maximum power is generated by the solar cell at a point of the current-voltage characteristic where the product VI is maximum. This point is known as the MPP and is unique, as can be seen in Figure 3, where the previous points are represented.

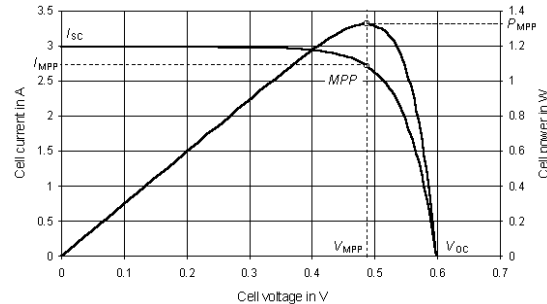


Figure 4: Important points in the characteristic curves of a solar panel.

2.4 Fill Factor

Using the MPP current and voltage, I_{MPP} and V_{MPP}, the open circuit voltage (V_{OC}) and the short circuit current (I_{SC}), the fill factor (FF) can be defined as:

$$FF = \frac{I_{MPP} \cdot V_{MPP}}{I_{SC} \cdot V_{OC}} \tag{4}$$

It is a widely used measure of the solar cell overall quality. It is the ratio of the actual maximum power (IMPPVMPP) to the theoretical one (ISCVOC), which is actually not obtainable. The reason for that is that the MPP voltage and current are always below the open circuit voltage and the short circuit current respectively, because of the series and shunt resistances and the diode depicted in Figure 2. The typical fill factor for commercial solar cells is usually over 0.70.

2.5 Temperature and irradiance effects

Two important factors that have to be taken into account are the irradiation and the temperature. They strongly affect the characteristics of solar modules. As a result, the MPP varies during the day and that is the main reason why the MPP must constantly be tracked and ensure that the maximum available power is obtained from the panel.

The effect of the irradiance on the voltage-current (V-I) and voltage-power (V-P) characteristics is depicted in Figure 4, where the curves are shown in per unit, i.e. the voltage and current are normalized using the VOC and the ISC respectively, in order to illustrate better the effects of the irradiance on the V-I and V-P curves. As was previously mentioned, the photo-generated current is directly proportional to the irradiance level, so an increment in the irradiance leads to a higher photo-generated current. Moreover, the short circuit current is directly proportional to the photo-generated current; therefore it is directly proportional to the irradiance. When the operating point is not the short circuit, in which no power is generated, the photo-generated current is also the main factor in the PV current, as is expressed by equations (1). For this reason the voltage-current characteristic varies with the irradiation. In contrast, the effect in the open circuit voltage is relatively small, as the dependence of the light generated current is logarithmic, as is shown in equation (4).

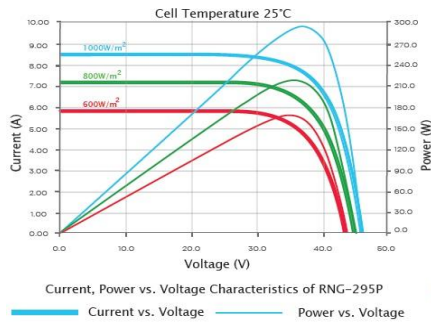


Figure 5: V-I and V-P curves at constant temperature (25°C) and three different isolation values

Figure 5 shows that the change in the current is greater than in the voltage. In practice, the voltage dependency on the irradiation is often neglected. As the effect on both the current and voltage is positive, i.e. both increase when the irradiation rises, the effect on the power is also positive: the more irradiation, the more power is generated.

The temperature, on the other hand, affects mostly the voltage. The open circuit voltage is linearly dependent on the temperature, as shown in the following equation:

$$V_{OC} = \frac{kT}{q} \ln \left(\frac{I_{SC}}{I_0} + 1 \right) \tag{5}$$

According to (5), the effect of the temperature on VOC is negative, because Kv is negative, i.e. when the temperature rises, the voltage decreases. The current increase with the temperature but very little and it does not compensate the decrease in the voltage caused by a given temperature rise. That is why the power also decreases. PV panel manufacturers provide in their data sheets the temperature coefficients, which are the parameters that specify how the open circuit voltage, the short circuit current and the maximum power vary when the temperature changes. As the effect of the temperature on the current is really small, it is usually neglected. Figure 6 shows how the voltage-current and the voltage-power characteristics change with temperature. The curves are again in per unit, as in the previous case.

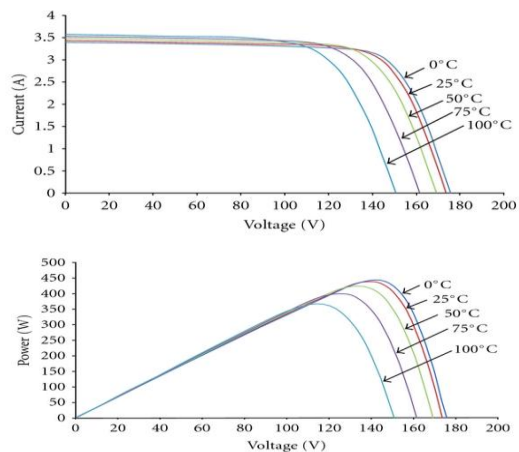


Figure 6: V-I and V-P curves at constant irradiation (1 kW/m²) and three different temperatures

As was mentioned before, the temperature and the irradiation depend on the atmospheric conditions, which are not constant during the year and not even during a single day; they can vary rapidly due to fast changing conditions such as clouds. This causes the MPP to move constantly, depending on the irradiation and temperature conditions. If the operating point is not close to the MPP, great power

losses occur. Hence it is essential to track the MPP in any conditions to assure that the maximum available power is obtained from the PV panel. In a modern solar power converter, this task is entrusted to the MPPT algorithms.

3. Buck-Boost Converter

The basic schematic of a buck-boost converter. Two different topologies are called buck-boost converter. Both of them can produce an output voltage much larger (in absolute magnitude) than the input voltage. Both of them can produce a wide range of output voltage from that maximum output voltage to almost zero.

- The inverting topology – The output voltage is of the opposite polarity as the input

A buck (step-down) converter followed by– boost (step-up) converter. The output voltage is of the same polarity as the input, and can be lower or higher than the input. Such a non-inverting buck-boost converter may use a single inductor that is used as both the buck inductor and the boost inductor.

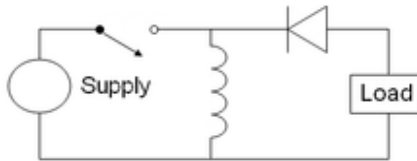


Figure 7: Buck-Boost Converter

This page describes the inverting topology. The buck-boost converter is a type of that has an output voltage magnitude that is either greater than or less than the input voltage magnitude. It is a switched-mode power supply with a similar circuit topology to the boost converter and the buck converter. The output voltage is adjustable based on the duty cycle of the switching transistor. One possible drawback of this converter is that the switch does not have a terminal at ground; this complicates the driving circuitry. Also, the polarity of the output voltage is opposite the input voltage. Neither drawback is of any consequence if the power supply is isolated from the load circuit (if, for example, the supply is a battery) as the supply and diode polarity can simply be reversed. The switch can be on either the ground side or the supply side.

3.1 Principle of operation:

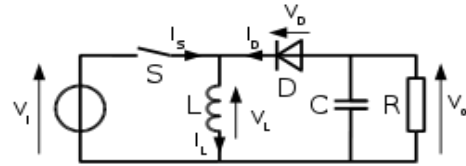


Figure 8: Schematic of a buck-boost converter

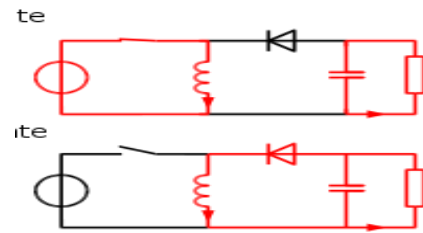


Fig. 9: The two operating states of a buck-boost converter

The basic principle of the buck-boost converter is fairly simple (see figure 2):

- While in the On-state, the input voltage source is directly connected to the inductor (L). This results in accumulating energy in L. In this stage, the capacitor supplies energy to the output load.
- While in the Off-state, the inductor is connected to the output load and capacitor, so energy is transferred from L to C and R.

Compared to the buck and boost converters, the characteristics of the buck-boost converter are mainly:

- Polarity of the output voltage is opposite to that of the input;
- The output voltage can vary continuously from 0 to $-\infty$ (for an ideal converter). The output voltage ranges for a buck and a boost converter are respectively 0 to V_i and V_i to ∞ .

3.2 Continuous Mode

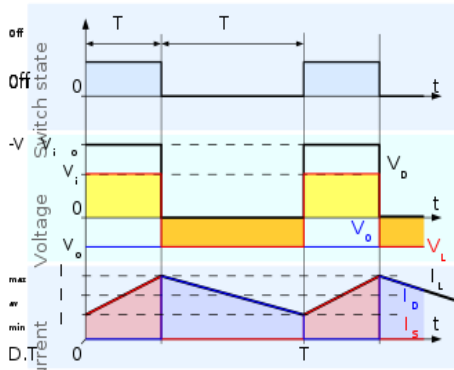


Figure 10: Waveforms of current and voltage in a buck-boost converter operating in continuous mode

If the current through the inductor L never falls to zero during a commutation cycle, the converter is said to operate in continuous mode. The current and voltage waveforms in an ideal converter can be seen in Figure 10.

From $t=0$ to $t=DT$, the converter is in On-State, so the switch S is closed. The rate of change in the inductor current (IL) is therefore given by , $\frac{dI_L}{dt} = \frac{V_i}{L}$

At the end of the On-state, the increase of IL is therefore:

$$\Delta I_{L_{On}} = \int_0^{DT} dI_L = \int_0^{DT} \frac{V_i}{L} dt = \frac{V_i DT}{L}$$

D is the duty cycle. It represents the fraction of the commutation period T during which the switch is On. Therefore D ranges between 0 (S is never on) and 1 (S is always on).

During the Off-state, the switch S is open, so the inductor current flows through the load. If we assume zero voltage drops in the diode, and a capacitor large enough for its voltage to remain constant, the evolution of IL is: $\frac{dI_L}{dt} = \frac{V_o}{L}$

Therefore, the variation of IL during the Off-period is: $\Delta I_{L_{Off}} = \int_0^{(1-D)T} dI_L = \int_0^{(1-D)T} \frac{V_o}{L} dt = \frac{V_o(1-D)T}{L}$

As we consider that the converter operates in steady-state conditions, the amount of energy stored in each of its components has to be the same at the beginning

and at the end of a commutation cycle. As the energy in an inductor is given by: $E = \frac{1}{2} L I_L^2$

It is obvious that the value of IL at the end of the Off state must be the same as the value of IL at the beginning of the On-state, i.e. the sum of the variations of IL during the on and the off states must be zero: $\Delta I_{L_{On}} + \Delta I_{L_{Off}} = 0$

Substituting $\Delta I_{L_{On}}$ and $\Delta I_{L_{Off}}$ by their expressions yields: $\Delta I_{L_{On}} + \Delta I_{L_{Off}} = \frac{V_i DT}{L} + \frac{V_o(1-D)T}{L} = 0$

$$\text{This can be written as: } \frac{V_o}{V_i} = \left(\frac{-D}{1-D} \right)$$

$$\text{This in return yields that: } D = \frac{V_o}{V_o - V_i}$$

From the above expression it can be seen that the polarity of the output voltage is always negative (as the duty cycle goes from 0 to 1), and that its absolute value increases with D, theoretically up to minus infinity as D approaches 1. Apart from the polarity, this converter is either step-up (as a boost converter) or step-down (as a buck converter). This is why it is referred to as a buck-boost converter.

3.3 Discontinuous Mode

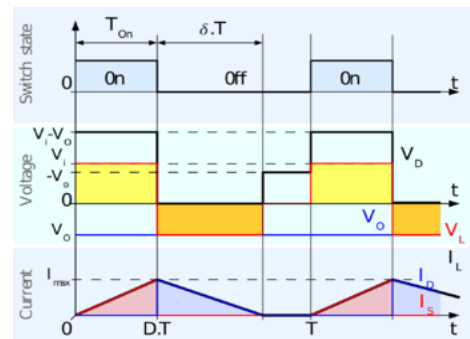


Figure11: Waveforms of current and voltage in a buck-boost converter operating in discontinuous mode

In some cases, the amount of energy required by the load is small enough to be transferred in a time smaller than the whole commutation period. In this case, the current through the inductor falls to zero during part of the period. The only difference in the principle described above is that the inductor is completely discharged at the end of the commutation cycle (see waveforms in figure 11). Although slight, the difference has a strong effect on the output voltage equation. It can be calculated as follows:

As the inductor current at the beginning of the cycle is zero, its maximum value $I_{L_{max}}$ (at $t = DT$) is

$$I_{L_{max}} = \frac{V_i DT}{L}$$

During the off-period, IL falls to zero after $\delta.T$:

$$I_{L_{max}} + \frac{V_o \delta T}{L} = 0$$

Using the two previous equations, δ is:

$$\delta = -\frac{V_i D}{V_o}$$

The load current I_o is equal to the average diode current (ID). As can be seen on figure 11, the diode current is equal to the inductor current during the off-state. Therefore, the output current can be written as:

$$I_o = \bar{I}_D = \frac{I_{L_{max}} \delta}{2}$$

Replacing $I_{L_{max}}$ and δ by their respective expressions yields:

$$I_o = -\frac{V_i DT V_i D}{2L V_o} = -\frac{V_i^2 D^2 T}{2L V_o}$$

Therefore, the output voltage gain can be written as:

$$\frac{V_o}{V_i} = -\frac{V_i D^2 T}{2L I_o}$$

Compared to the expression of the output voltage gain for the continuous mode, this expression is much more complicated. Furthermore, in discontinuous operation, the output voltage not only depends on the duty cycle, but also on the inductor value, the input voltage and the output current.

3.4 Limit between continuous and discontinuous modes:

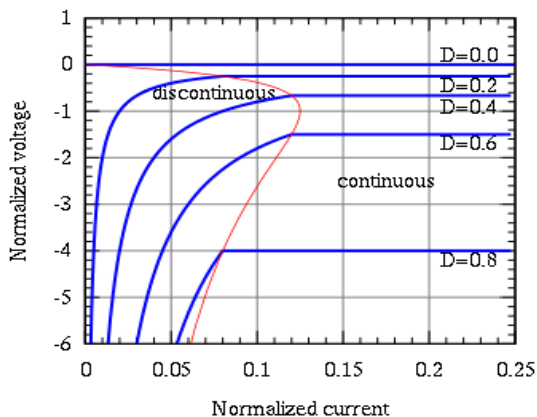


Figure 12: Evolution of the normalized output voltage with the normalized output current in a buck-boost converter

As told at the beginning of this section, the converter operates in discontinuous mode when low current is drawn by the load, and in continuous mode at higher load current levels. The limit between discontinuous and continuous modes is reached when the inductor current falls to zero exactly at the end of the commutation cycle. With the notations of figure 11, this corresponds to:

$$DT + \delta T = T \quad \text{and} \quad D + \delta = 1$$

In this case, the output current $I_{o_{lim}}$ (output current at the limit between continuous and discontinuous modes) is given by:

$$I_{o_{lim}} = \bar{I}_D = \frac{I_{L_{max}}}{2} (1 - D)$$

Replacing $I_{L_{max}}$ by the expression given in the discontinuous mode section yields:

$$I_{o_{lim}} = \frac{V_i DT}{2L} (1 - D)$$

As $I_{o_{lim}}$ is the current at the limit between continuous and discontinuous modes of operations, it satisfies the expressions of both modes. Therefore, using the expression of the output voltage in continuous mode, the previous expression can be written as:

$$I_{o_{lim}} = \frac{V_i DT V_i}{2L V_o} (-D)$$

Let's now introduce two more notations:

- The normalized voltage, defined by $|V_o| = \frac{V_o}{V_i}$. It corresponds to the gain in voltage of the converter;
- The normalized current, defined by $|I_o| = \frac{L}{T V_i} I_o$. The term $\frac{T V_i}{L}$ is equal to the maximum increase of the inductor current during a cycle; i.e., the increase of the inductor current with a duty cycle $D=1$. So, in steady state operation of the converter, this means that $|I_o|$ equals 0 for no output current, and 1 for the maximum current the converter can deliver.

Using these notations, we have:

- in continuous mode, $|V_o| = -\frac{D}{1-D}$;
- in discontinuous mode, $|V_o| = -\frac{D^2}{2|I_o|}$;

The current at the limit between continuous and discontinuous mode

is $I_{o1im} = \frac{V_i T}{2L} D(1-D) = \frac{I_{o1im}}{2|I_o|} D(1-D)$. Therefore the locus of the limit between continuous and discontinuous modes is given by $\frac{1}{2|I_o|} D(1-D) = 1$.

4. ANALYSIS OF AT89S52 :

The AT89S52 is a low-power, high-performance CMOS 8-bit microcontroller with 8K bytes of in-system programmable Flash memory. The device is manufactured using Atmel’s high-density non-volatile memory technology and is compatible with the industry-standard 80C51 instruction set and pin-out. The on-chip Flash allows the program memory to be reprogrammed in-system or by a conventional non-volatile memory programmer. By combining a versatile 8-bit CPU with in-system programmable Flash on a monolithic chip, the Atmel AT89S52 is a powerful microcontroller which provides a highly-flexible and cost-effective solution to many embedded control applications.

The AT89S52 provides the following standard features: 8K bytes of Flash, 256 bytes of RAM, 32 I/O lines, Watchdog timer, two data pointers, three 16-bit timer/counters, a six-vector two-level interrupt architecture, a full duplex serial port, on-chip oscillator, and clock circuitry. In addition, the AT89S52 is designed with static logic for operation down to zero frequency and supports two software selectable power saving modes. The Idle Mode stops the CPU while allowing the RAM, timer/counters, serial port, and interrupt system to continue functioning. The Power-down mode saves the RAM contents but freezes the oscillator, disabling all other chip functions until the next interrupt or hardware reset.

T2/P1.0	1	40	Vcc
T2EX/P1.1	2	39	P0.0/AD0
P1.2	3	38	P0.1/AD1
P1.3	4	37	P0.2/AD2
P1.4	5	36	P0.3/AD3
MOSI/P1.5	6	35	P0.4/AD4
MISO/P1.6	7	34	P0.5/AD5
SCK/P1.7	8	33	P0.6/AD6
RST	9	32	P0.7/AD7
RXD/P3.0	10	31	EA/VPP
TXD/P3.1	11	30	ALE/PROG
INT0/P3.2	12	29	PESH
INT1/P3.3	13	28	P2.7/A15
T0/P3.4	14	27	P2.6/A14
T1/P3.5	15	26	P2.5/A13
WR/P3.6	16	25	P2.4/A12
RD/P3.7	17	24	P2.3/A11
XTAL2	18	23	P2.2/A10
XTAL1	19	22	P2.1/A9
PDIP	20	21	P2.0/A8
GND			

Figure 13: AT89S52

5. Advanced Power Mosfet IRFZ44N:

It is a voltage controlled device and developed by combining the area of field-effect concept and MOS technology. It has 3 terminals called drain (D), source(S) and gate (G). Due to higher mobility of electrons n-channel enhancement MOSFET is used. It utilizes advanced processing techniques to achieve extremely low on-resistance per silicon area. This benefit, combined with the fast switching speed and rugged zed device design that power MOSFETs are well known for, provided the designer with an extremely efficient and reliable device for use in a wide variety of applications. The T0-220 package is universally preferred foe all commercial-industrial applications at power dissipation levels to approximately 50 watts. The low thermal resistance and low package cost of the T0-220 contribute to its wide acceptance.

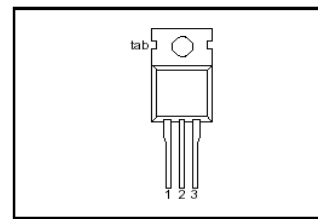


Figure 14: IRFZ44N Mosfet Diagram

PIN	DESCRIPTION
1	gate
2	drain
3	source
tab	drain

Table 1: Connection of IRFZ44N Mosfet

- VDSS = 55V
- RDS(on) = 17.5mΩ
- ID = 49A

6. PWM METHODS

6.1 Sine PWM

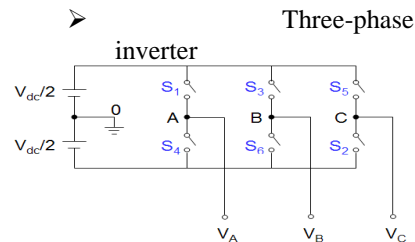


Figure 15: Three-phase Sine PWM inverter

- Three-phase sine PWM waveforms
 - Frequency of v_{tri} and $v_{control}$
 - Frequency of $v_{tri} = f_s$
 - Frequency of $v_{control} = f_l$

Where, f_s = PWM frequency

f_l = Fundamental frequency

- Inverter output voltage
 - When $v_{control} > v_{tri}$, $V_{A0} = V_{dc}/2$
 - When $v_{control} < v_{tri}$, $V_{A0} = -V_{dc}/2$

Where, $V_{AB} = V_{A0} - V_{B0}$
 $V_{BC} = V_{B0} - V_{C0}$
 $V_{CA} = V_{C0} - V_{A0}$

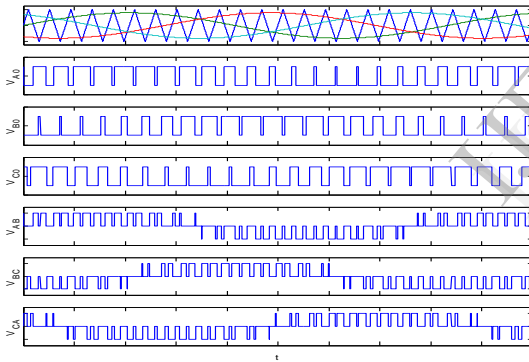


Figure 16: Waveforms of three-phase sine PWM inverter

- Amplitude modulation ratio (ma)

$$\therefore m_a = \frac{\text{peak amplitude of } v_{control}}{\text{amplitude of } v_{tri}} = \frac{\text{peak value of } (V_{A0})_1}{V_{dc}/2}$$

where, $(V_{A0})_1$: fundamental frequency component of V_{A0}

- frequency modulation ratio (mf)

$$m_f = \frac{f_s}{f_l}, \text{ where, } f_s = \text{PWM frequency and } f_l = \text{fundamental frequency}$$

- f should be an odd integer
 - f m_f is not an integer, there may exist some harmonics at output voltage
 - f m_f is not odd, DC component may exist and even harmonics are present at output voltage
- f should be a multiple of 3 for three-phase PWM inverter
 - n odd multiple of 3 and even harmonics are suppressed

6.2 Hysteresis (Bang-bang) PWM

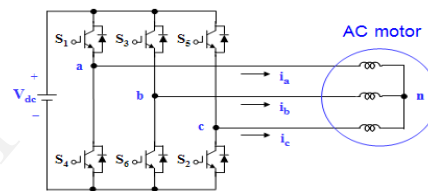


Figure 17: Three-phase inverter for hysteresis current control

- Hysteresis Current Controller

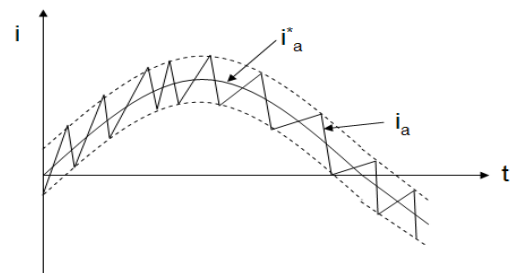
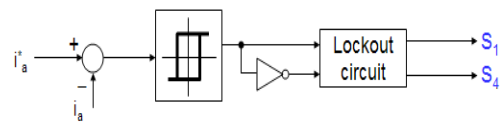


Figure 18: Hysteresis current controller at Phase "a"

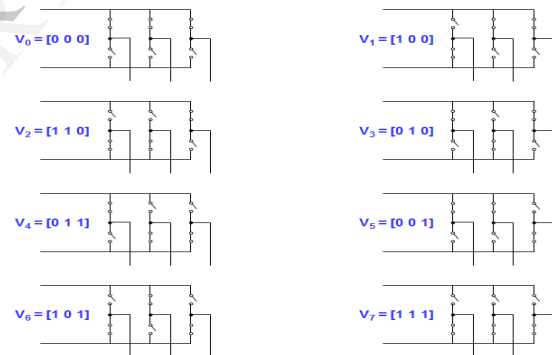
➤ **Characteristics of hysteresis Current Control**

- Advantages
 - Excellent dynamic response
- Low cost and easy implementation
- Drawbacks
 - Large current ripple in steady-state
 - Variation of switching frequency
 - No intercommunication between each hysteresis controller of three phases and hence no strategy to generate zero-voltage vectors. As a result, the switching frequency increases at lower modulation index and the signal will leave the hysteresis band whenever the zero vector is turned on.
 - The modulation process generates sub-harmonic component



Output voltages of three-phase inverter

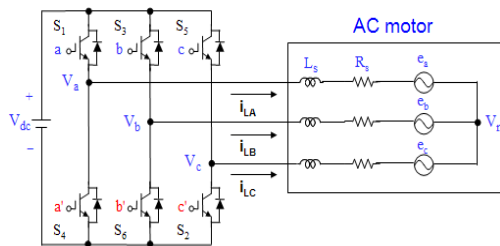
- S1 through S6 are the six power transistors that shape the output voltage
- When an upper switch is turned on (i.e., a, b or c is “1”), the corresponding lower switch is turned off (i.e., a', b' or c' is “0”)
- Line to line voltage vector $[V_{ab} \ V_{bc} \ V_{ca}]^T$
- Line to neutral (phase) voltage vector $[V_{an} \ V_{bn} \ V_{cn}]^T$
- The eight inverter voltage vectors (V0 to V7)



6.3 Space Vector PWM (1)



Three-phase inverter



Where, Upper transistors: S1, S3, S5

Lower transistors: S4, S6, S2

Switching variable vector: a, b, c

Figure 19: Three-phase power inverter

The eight combinations, phase voltages and output line to line voltages

Voltage Vectors	Switching Vectors			Line to neutral voltage			Line to line voltage		
	a	b	c	V_{an}	V_{bn}	V_{cn}	V_{ab}	V_{bc}	V_{ca}
V ₀	0	0	0	0	0	0	0	0	0
V ₁	1	0	0	2/3	-1/3	-1/3	1	0	-1
V ₂	1	1	0	1/3	1/3	-2/3	0	1	-1
V ₃	0	1	0	-1/3	2/3	-1/3	-1	1	0
V ₄	0	1	1	-2/3	1/3	1/3	-1	0	1
V ₅	0	0	1	-1/3	-1/3	2/3	0	-1	1
V ₆	1	0	1	1/3	-2/3	1/3	1	-1	0
V ₇	1	1	1	0	0	0	0	0	0

(Note that the respective voltage should be multiplied by V_{dc})

7. SIMULATION:

7.1 SOLAR PANEL:

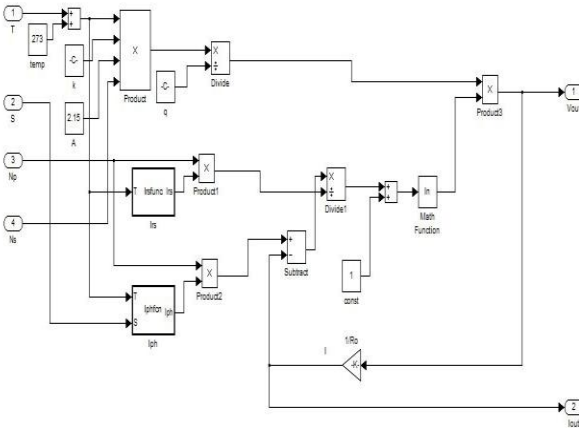


Figure 20: Unmasked block diagram of the modelled solar PV panel

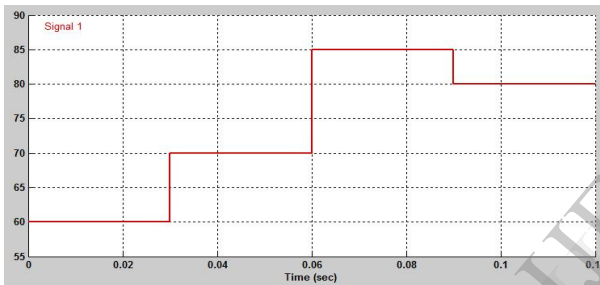


Figure 21: Irradiation signal (Watt/sq. cm. versus time)

7.3 FINAL SIMULATION:

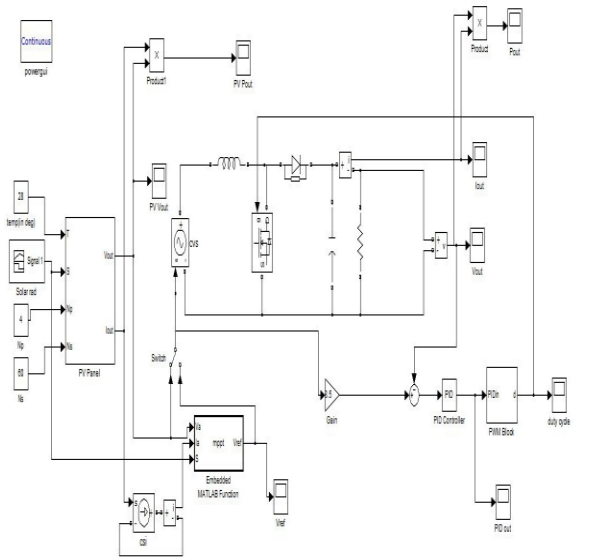


Figure 22: SIMULINK™ Model of MPPT system using P&O algorithm

7.3.1 RUNNING THE SYSTEM WITHOUT MPPT:

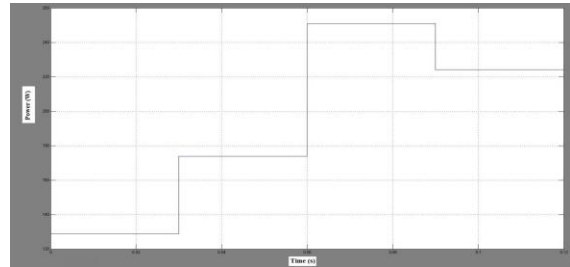


Figure 23: Plot of Power output of PV panel v/s time without MPPT

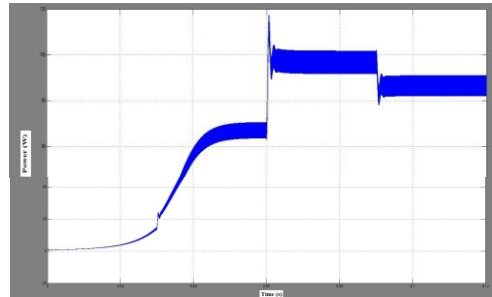


Figure 24: Plot of Power obtained at load side v/s time without MPPT

7.3.2 RUNNING THE SYSTEM WITH MPPT:

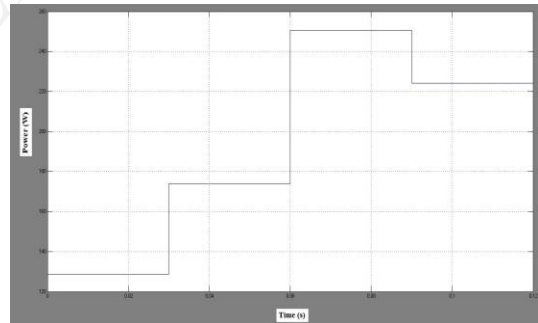


Figure 25: Plot of Power output of PV panel v/s time with MPPT

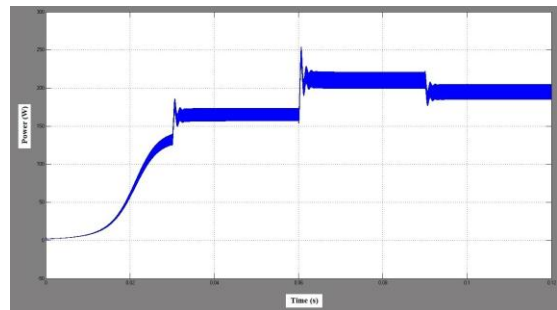


Figure 26: Plot of Power obtained at load side v/s time with MPPT

8. CONCLUSION

A renewable energy system, like the one implemented here, is suitable for residential and/or industrial applications. The results suggest that, on the basis of maximum power point tracking efficiency, the perturb-and-observe method, already by far the most commonly used algorithm in commercial converters, has the potential to be very competitive with other methods if it is properly optimized for the given hardware.

Thus a system such as this can be deployed easily with little concern about adapting a home or business's electrical wiring to take advantage of solar energy. Many areas allow surplus energy generated by systems such as this to be sold to the utility grid in a policy known as "net metering."

After accomplishing the model of PV modules, the models of DC-DC buck-boost converter and MPPT systems are combined with it to complete the PV simulation system with the MPPT function. The accuracy and execution efficiency for each MPPT algorithm can then be simulated under different weather voltage.

Therefore, it was seen that using the Perturb & Observe MPPT technique increased the efficiency of the photovoltaic system by approximately 126% from an earlier output power.

REFERENCES

1. Dylan D .C. Lu , R.H. Chu, S. sathiakumar & V.G Agilides , "A Converter with simple Maximum Power Point Tracking for Power Electronics Education On Solar Energy System" in IEEE trans. On power electronics
 2. S. B. Kjaer, J. K. Pedersen, and F. Blaabjerg, "A Review of Single-Phase Grid-Connected Inverters for Photovoltaic Modules," in IEEE Trans. on Power Electron., Vol. 41, No. 5, pp. 1292–1306, Sep./Oct. 2005
 3. Power Electronics: Circuits, Devices and Operations (Book) - Muhammad H. Rashid
 4. Power Electronics (Book) –Dr. P.S. Bimbhra
 5. Resource and Energy Economics - C Withagen - 1994 – Elsevier
 6. Advanced Algorithm for control of Photovoltaic systems - C. Liu, B. Wu and R. Cheung
- Webpage:
<http://en.wikipedia.org/wiki/buck-boost>
 - Webpage:
<http://en.wikipedia.org/wiki/solarcell>